

# Chapter 1 Introduction

The last few years have seen the beginning of a new era in high dynamic range seismic instrumentation. 24-bit resolution (which translates to  $\sim 7$  orders of magnitude) is now commonplace and becoming readily affordable. It is the standard for many seismic networks, and is increasingly common in engineering networks. Instruments are now designed to record over a wide frequency range to take advantage of this new resolution. It is also increasingly possible for networks to store large volumes of high sample rate continuous data at reasonable cost with relative ease. This thesis examines new research that has only become possible with the wealth of data that has recently become available to the community.

Two main issues are dealt with in this thesis:

1. What is the current system of seismological instrumentation. How does it work, how does it overlap, and how can it be improved?
2. What new applications are now possible with the modern instrumentation?

In addressing these issues, the following problems are explored:

- a. understanding the best instrumentation for recording ground motions over the widest possible band of interest.
- b. prediction of motions of a tall building structure from small motions of a nearby free-field station.
- c. removing the total path effect from earthquake records: isolating which part of a record is due to the source, and then what can be learned from this source time function.

## 1.1 Seismological Instrumentation

Chapter 2 describes the typical specifications of a modern broadband seismic network station, using the California Integrated Seismic Network as an example. The benefits of introducing a strong motion velocity recording instrument in place of the accelerometer are

discussed.

In Chapter 3, an existing strong motion instrument with widespread usage in Japan is introduced, and a regime of laboratory tests is described which shows whether the instrument is capable of performing to the levels anticipated in Chapter 2. A major design flaw was exposed during the tests; the instrument as delivered was observed to be incapable of resolving strong motions above  $15\text{cm/s}$ , well below the advertised clip level of  $200\text{cm/s}$ , and the expected motions in the near field of large earthquakes.

Nonetheless, many of these instruments are deployed in modern networks in Japan, and were heavily excited by the shaking produced during the 25 September 2003 M8.3 Tokachi-Oki earthquake, located offshore of Hokkaido Island in Japan. The data produced during this event provided a dataset allowing a thorough analysis of the quality of data one may expect from the strong motion velocity instrument, and provides the basis for Chapter 4. Unfortunately, the problems observed in the laboratory experiments, documented in Chapter 3, were also observed in the field.

Widespread static offsets over hundreds of square kilometres also exposed the inability of the strong motion velocity sensor to improve on accelerometer recordings of static offset. Chapter 4 shows that recording high-rate GPS displacement alongside a strong motion instrument is very important if wide-band,  $100\text{Hz}$  — DC displacements are to be accurately recorded. The usefulness of the strong motion instrument in the network is also observed as motions saturate some sensors at up to  $1000\text{km}$  distance. Network-wide individual station health monitoring can also be performed by comparing the signals from the 2 co-located broadband and strong motion sensors during such large magnitude earthquakes.

In Chapter 5, modifications to the strong motion instrument are documented, as are the results of laboratory tests on this new instrument, which indicate the sensor now operates to the specifications first advertised.

## 1.2 Applications of Modern Instrument Data

### 1.2.1 Small Amplitude Studies for Buildings

When attempting to predict motions of a tall building structure from small motions of a nearby free-field station, the problem of how a structure's natural periods vary is fundamentally important. Small variations in this parameter have important consequences not only in modelling the structural response to ground motion, but also in determining the building stiffness.

Whilst there is a wealth of knowledge and research concerning structural dynamics, the earth-building system in general is not well understood. Chapter 6 investigates the question of whether the response of a building during strong motions can be predicted solely from knowing the response at a local base station. The installation of a 24-bit continuously recording accelerometer station within the California Integrated Seismic Network (CISN) on the 9<sup>th</sup> floor of Caltech's Millikan Library, alongside other nearby ground CISN stations, facilitated this investigation.

### 1.2.2 Moderate Earthquake Source Inversions

Focal mechanism solutions are rapidly produced for many earthquakes recorded in the Southern California. The focal mechanism represents the orientation of the point source that best fits either the hypocentral motions (first motion solution) or the overall earthquake (moment tensor solution). If the source is constrained to be a double couple, then the plane of rupture can be either of the two conjugate planes described by this solution. Of course earthquakes will have a finite rupture area and consequently some directivity pattern. Knowing the pattern of the directivity can determine which plane on the focal sphere a rupture occurs on. Unfortunately, path and station effects obscure this directivity for even moderately large events ( $M < 6$ ). Chapter 7 introduces a method of deconvolving a 'point source' aftershock from the mainshock, which can provide an estimate of the source-time function of an earthquake, and indicate the directivity of the mainshock. An aftershock with the same epicentral location and focal mechanism as the mainshock is selected, which

will then have the same radiation pattern, path and site effects as the mainshock. This study is only possible with the quality (in particular the dynamic range) and density of stations in the CISON, which allows recordings of the mainshock and aftershocks at many stations with good signal to noise.

### 1.3 A Comment on Deconvolutions

This thesis includes various methods of solving the problem of deconvolution. The convolution operation,  $*$ , is a linear operator between two functions  $G(t)$  and  $u(t)$ , and may be written as

$$x(t) = G(t) * u(t) \quad (1.1)$$

$$x(t) = \int_{-\infty}^{\infty} G(\tau)u(t - \tau) d\tau \quad (1.2)$$

where  $x(t)$  is the convolution of the functions  $G(t)$  and  $u(t)$ . In this work, the independent variable,  $t$ , will always refer to time.

An important property of the convolution operator is that its conjugate operator in the frequency domain is simply the multiplication operator. So

$$X(\omega) = G(\omega)U(\omega) \quad (1.3)$$

where  $X(\omega)$ ,  $G(\omega)$  and  $U(\omega)$  are the Fourier Transforms of  $x(t)$ ,  $G(t)$  and  $u(t)$ , respectively, and  $\omega$  is frequency.

[In practice, a discrete version of a Fourier Transform, the Fast Fourier Transform, or FFT, is used. The discrete inverse function is the Inverse Fast Fourier Transform, or IFFT.]

In Chapters 2-4, timeseries obtained from different seismometers will be analysed. In this case,  $x(t)$  is the observed seismometer output, and  $u(t)$  is the ground displacement, which when convolved with the instrument impulse response, or Green's function,  $G(t)$ , gives  $x(t)$ . In the frequency domain,  $G(\omega)$  is known as the Transfer Function of the instrument. The problem is to recover the ground displacement by deconvolving it from the

known instrument response.

Due to the characteristics of the instrument response of broadband sensors, the output from a particular seismometer may be simple over a particular frequency range (i.e.,  $G(\omega)$  within this frequency range is not sensitive to frequency, and is a constant value). However, when considering very broadband signals, the instrument response is sensitive to frequency, and must be removed. This problem is traditionally performed in the frequency domain, where the Fourier Transform of the timeseries,  $X(\omega)$ , is divided by the Transfer Function  $G(\omega)$  to get the FFT of the ground displacement,  $U(\omega)$ .  $u(t)$  is then obtained by an IFFT

$$u(t) = IFFT \left[ \frac{X(\omega)}{G(\omega)} \right] \quad (1.4)$$

A problem arises for broadband strong motion velocity instruments, where motions are large, records are short, and static offsets are expected. The frequency domain method does not give physically realistic solutions, as displacements and velocities must be zero before the earthquake occurs. Further, division in the frequency domain requires a high pass filter at low frequency to prevent numerical instability (division by zero). This removes the static offset. In this case a different approach to deconvolving the instrument response from the ground displacement is required— a time domain solution employing direct integration of the equivalent equation of motion for the sensor system is used

$$\ddot{x}(t) + 2\beta\dot{x}(t) + \omega_0^2 x(t) = G\ddot{u}(t) \quad (1.5)$$

These parameters will be defined in Chapter 3. Direct integration leads to

$$u(t) = \frac{1}{G} \left( \int x(t) dt + 2\beta \iint x(t) dt^2 + \omega_0^2 \iiint x(t) dt^3 \right) - At^2/2 - Bt - C \quad (1.6)$$

where  $A$ ,  $B$  and  $C$  are constants of integration determined by initial conditions.

As  $t$  becomes large, the solution becomes unstable due to tilts and other sources of small trends in the record, but this is often not significant in the short duration of a strong motion record.

Finally, in Chapter 7, the problem of removing the path effects from a seismogram is

discussed using empirical Green's Functions. An earthquake timeseries on an instrument recording,  $x(t)$ , can be approximated as the convolution of response time functions from the source,  $S(t)$ , the path,  $P(t)$ , the site,  $C(t)$  and the instrument,  $I(t)$

$$x_m(t) \approx S_m(t) * P_m(t) * C_m(t) * I_m(t) \quad (\text{mainshock}) \quad (1.7)$$

$$x_a(t) \approx S_a(t) * P_a(t) * C_a(t) * I_a(t) \quad (\text{aftershock}) \quad (1.8)$$

It is assumed that a small aftershock, with similar focal mechanism to the mainshock, has a  $\delta$ -function as source time function. If the mainshock and aftershock have a similar focal mechanism and location, then the path, site and instrument responses should be the same for both  $x_m(t)$  and  $x_a(t)$ . Thus, one can assume

$$x_m(t) \sim S_m(t) * x_a(t) \quad (1.9)$$

The source time function of the mainshock,  $S_m(t)$ , can be approximated as the deconvolution of the aftershock time function from the mainshock time function. Solving this in the frequency domain requires a division by  $X_a(\omega)$ , which will cause instabilities as earthquakes timeseries have many near-zero amplitudes in the frequency domain. Thus an approach in the time domain is employed, using the definition of deconvolution (Equation 1.2) written as a series of vectors (outlined in Bracewell (1965)). As shown in the following set of equations, the convolution operator may be described as a matrix multiplication, with the matrix defined by the aftershock timeseries —

The 3 functions of Equation 1.9 can be written as

$$x_{m_i} = x_m(i\Delta t), \quad i = 0, n_1 \quad (1.10)$$

$$x_{a_i} = x_a(i\Delta t), \quad i = 0, n_2 \quad (1.11)$$

$$S_m = S_m(i\Delta t), \quad i = 0, (n_1 - n_2) + 1 \quad (1.12)$$

and so the convolution in Equation 1.9 may be written as the serial product

$$x_{m_i} = (S_m * x_{a_i})_i = \sum_{j=1}^{n_1} S_{m_j} x_{a_{i-j}} \Delta t \quad (1.13)$$

and the serial product can be re-written in matrix form, expanding  $x_a$

$$\Delta t \begin{bmatrix} x_{a_0} & 0 & 0 & \dots & 0 \\ x_{a_1} & x_{a_0} & 0 & \dots & 0 \\ x_{a_2} & x_{a_1} & x_{a_0} & \dots & 0 \\ \vdots & \vdots & \vdots & \ddots & \vdots \\ x_{a_{n_2}} & x_{a_{n_2-1}} & x_{a_{n_2-2}} & \dots & x_{a_{n_1}} \\ 0 & x_{a_{n_2}} & x_{a_{n_2-1}} & \dots & x_{a_{n_1+1}} \\ \vdots & \vdots & \vdots & \ddots & \vdots \\ 0 & 0 & 0 & \dots & x_{a_{n_1-n_2}} \end{bmatrix} \begin{pmatrix} S_{m_1} \\ S_{m_2} \\ S_{m_3} \\ \vdots \\ S_{m_{n_1-n_2+1}} \end{pmatrix} = \begin{pmatrix} x_{m_1} \\ x_{m_2} \\ x_{m_3} \\ \vdots \\ x_{m_{n_1}} \end{pmatrix} \quad (1.14)$$

which is now in the form

$$[A]\{y\} = \{b\} \quad (1.15)$$

where  $[A]$  is an  $n_1 \times (n_2 - n_1 + 1)$  matrix.

The deconvolution has now been re-written as a simple linear matrix inversion. Classical inversion techniques can be used to invert for the source time function vector,  $x$ . In Chapter 7, a damped least squares solution is used.

## 1.4 A Comment on Tilt

In many cases of strong motion, tilt is associated with heavy shaking, especially when static offsets are also present. Unfortunately, no matter what type of inertial instrument is used, whether an accelerometer, or a strong motion velocity-meter, tilt cannot be easily distinguished and removed from estimates of static offset, or indeed the true ground acceleration.

In strong motions, tilt can be caused by rotation of the ground due to tectonic displacements over a wide area, or can also be from local site failure, such as lateral spreading, or

liquefaction. It can also occur if the instrument shifts during a strong motion. The effect of tilt is to produce an offset in the acceleration timeseries. This offset can also be caused by an instrument malfunction, as has been observed for the FBA-23 (Iwan et al, 1985; Boore, 2001).

It is important to try to estimate the amount of tilt in a record. In a large thrust earthquake, there will be a tectonic tilt, which can affect the sensitive instruments. This tectonic tilt can be obtained from GPS.

To obtain the approximate tectonic tilt in a region, the change in elevation during the earthquake from 2 regional GPS stations,  $A$  and  $B$ , of known distance apart,  $L$ , is required ( $\Delta Z_A$  and  $\Delta Z_B$ ). The relative change in vertical displacement between the two stations is determined,  $\Delta Z_{A-B} = \Delta Z_A - \Delta Z_B$ , and the tectonic tilt,  $\theta_T$  is then

$$\theta_T = \frac{\Delta Z_{A-B}}{L} \quad (1.16)$$

The tilt measured from the seismometers,  $\theta_S$ , can be determined using the static offset at the end of an acceleration trace  $\Delta_{accn}$ , which can often be seen more clearly as the slope of the velocity trace (see Figure 3.6). The change in acceleration due to a tilt is simply  $\Delta_{accn} = g \sin(\theta_S)$  for horizontal channels, and  $\Delta_{accn} = g \cos(\theta_S)$  for the vertical channel, where  $g$  is the acceleration due to gravity,  $981 \text{ cm/s}^2$ . This is summarised in Figure 1.1. Assuming small angles of tilt,  $\sin(\theta_S) \sim \theta_S$ ,  $\cos(\theta_S) \sim 1 - \theta_S^2$  — note there is generally no observed change to the vertical channels during small tilts —  $\theta_S$  can then be measured from the horizontal channels as

$$\theta_S = \frac{\Delta_{accn}}{g} \quad (1.17)$$

If the tectonic tilt and the seismic tilt are of similar order of magnitude, then the tilt can be ascribed to the tectonic shift. Unfortunately, as was observed in the field for the M8.3 Tokachi-Oki earthquake in Japan, tilts in practice are typically far larger than that of the tectonic tilt. For stations located on poorer foundations (see Chapter 4 for data from the K-Net and WISE networks), the large tilts may be due to a local site failure such as liquefaction or lateral spreading. A further complication of this interpretation (illustrated in examples in Chapter 4), is that the largest permanent offsets often occur in the vertical



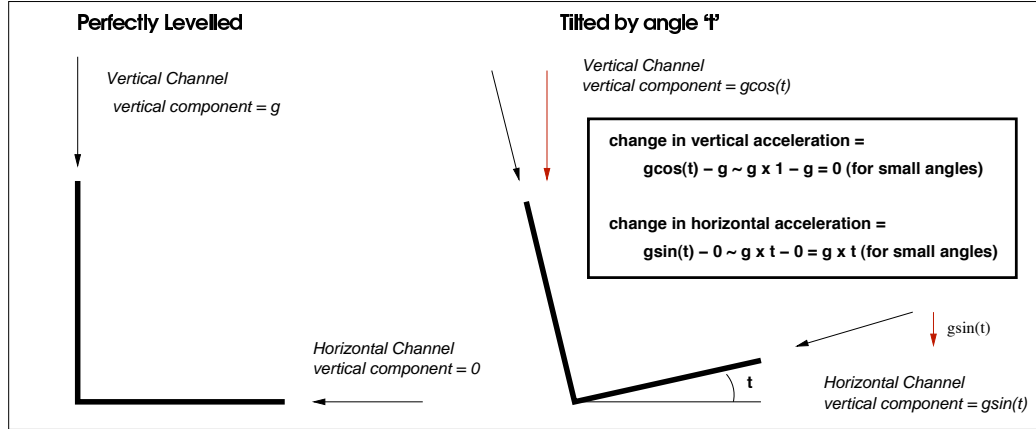


Figure 1.1: The effect of tilt on inertial seismometers.

acceleration timeseries. For tilting, the maximum changes are expected on the horizontal channels. Therefore, these examples strongly imply non-linear instrument behaviour.

Co-locating high sample rate GPS ( $\geq 1\text{ sps}$ ) and an inertial seismometer may indeed be the optimal method to obtain a true representation of the ground movement at a site. Preliminary data from high rate GPS in Hokkaido Island will be used to demonstrate the potential of a station of this type.

Finally, an example of the sensitivity of an instrument to tilt is as follows: Assume a site undergoes an instantaneous tilt of magnitude  $\theta$  about the N-S axis at time  $t = 0$ . The acceleration recorded by the E-W horizontal channel will be

$$a(t) = \ddot{u}(t) = g\theta \quad (1.18)$$

The N-S acceleration will be zero, as will the vertical acceleration if the tilt is small. The resultant E-W displacement is thus

$$u(t) = g\theta t^2/2 \quad (1.19)$$

Thus the rotation, or tilt, required to produce an error of only 5cm of displacement after

100s of an accelerometer record, is

$$\theta = \frac{5 \times 2}{981 \times 100^2} \quad (1.20)$$

$$= 1.02 \times 10^{-6} \text{ rads} \quad (1.21)$$

$$= 0.000058^\circ \quad (1.22)$$

So a tilt of only  $1 \mu\text{rad}$  will cause an error in the acceleration timeseries large enough to distort the true offset in displacement.

## 1.5 A Simple Methodology for Determining Displacement and Tilt Using Seismometers and GPS

Networks of GPS sensors are now commonplace in regions with plate boundaries. Measuring differential motion over the region gives important insight into the build-up of strain on faults. The movements of the plate boundaries drive the earthquake process, and so GPS networks and seismic networks tend to be located in the same region.

GPS is primarily installed to measure data at very long periods. Seismic data is insensitive to these extremely long period motions, with sensors designed to measure transient phenomena of short duration. With strong motion seismic sensors, it is difficult to resolve motions over 100s in duration.

In the past few years GPS displacement estimates have greatly improved, due to improvements in satellite infrastructure and number, developments in sensor placement and design, and better location algorithms. These improvements have also made it feasible to record GPS measurements at higher sampling rates. Current GPS sensors are capable of recording at up to  $10 \text{ sps}$  (though practitioners have questioned whether this data is useful). Many networks are recording data at  $1 \text{ sps}$ , with accuracy of about  $2 \text{ mm}$  for the horizontal components, slightly less accurate for the vertical.

The different optimal location requirements, as well as the independent goals of the networks, mean seismic and GPS stations are rarely co-located. In Southern California,

this is beginning to change, with co-location of 2 new CISN (California Integrated Seismic Network) and SCIGN (Southern California Integrated GPS Network) stations (recording high rate GPS) which traverse the San Andreas Fault. GPS stations require a clear view of the sky, as well as good foundations, preferably bedded on hard rock. An important requirement for a seismic station is low noise levels, and so many stations are located on hard rock and sensors may also be buried. In practice, co-location of seismic sensors and GPS does not require the instruments to be as close as possible, since records from Tokachi-Oki shows useful data can be recovered even when the sensors are separated by *1km*.

*1sps* high rate GPS Data from the M8.3 Tokachi-Oki earthquake was recorded for the entire GEONET network. Fortunately, the dense networks of both GPS and strong motion have overlap and some stations are very near each other.

Many investigators have tried to constrain seismic strong motion records using GPS offsets (Boore, 2001). The final co-seismic offset as measured from nearby GPS is used as a guide in determining the amount of tilt, as well as the onset of tilt. A similar approach with high-rate GPS data is possible, and can prove to be significantly more useful than the static offset alone. Previous studies were hampered by the fact the GPS stations were on the order of kilometers away from the seismic stations, so confidence in the correlation of the final offsets was low.

If the seismic and GPS stations are co-located, the permanent offset can be used to constrain the final offsets, and as *1sps* data is shown in this thesis to reproduce seismic motions with periods greater than *2s*, the GPS can also constrain the onset and magnitude of tilting.

It is noted in this work that in order to optimally match the seismic arrivals, and the magnitudes of the motion, there is a need to match orientations of the horizontal seismic sensors to the GPS timeseries. In data analysed in Chapter 4, a station was shown to require a vertical rotation of over  $30^\circ$ . Once this rotation has been made (if required), the two datasets can be inverted to solve for the three translations and two horizontal rotations. This is optimally done in the frequency domain, where the long period and static offsets from the GPS can be made to fully match the translational displacements, combining this

with the high frequency response of the inertial sensor. A damped least squares linear inversion with constraints can be used to determine the solution.

The inversion can simply be performed on each of the 2 horizontal components separately, or can include all the 3 components from the GPS and seismic sensor at once, which would use all the data available, though would also include any non-physical tilts observed in the vertical channel.

## 1.6 A Summary of Recommendations for Modern Station Design

The analysis in this section assumes all inertial sensors are near  $144dB$  quality, and are recording onto a 24-bit datalogger, unless otherwise stated.

The particular sensor options for a modern network station are

- high-gain broadband velocity sensor (e.g., STS-2)
- low-gain strong motion velocity sensor (e.g., VSE-355G3)
- low-gain strong motion force balance accelerometers (e.g., FBA-23, EpiSensor)
- GPS

All seismic sensors are theoretically sensitive to motions ranging from  $\sim 50Hz$  to DC. In reality the seismic sensors have optimal frequency ranges that do not encompass this entire range. GPS sensors record from  $1Hz$  (potentially up to  $10Hz$ ) to DC.

A summary of the sensor performance is as follows:

**GPS:** poor resolution at high frequency ( $1sps - 10sps$  sampling interval), insensitive to motions below  $2mm$  in horizontal channels,  $4mm$  vertical. Does not clip, and is not sensitive to tilt.

**high-gain broadband** [e.g., STS-2]: no strong motion as clip levels are about  $1cm/s$ , difficult calibration, poor high frequency resolution beyond  $20Hz$ .

**low-gain broadband** [e.g., VSE-355G3]: no restraint on tilt, complex transfer function response, difficult calibration.

**accelerometer** [e.g., EpiSensor]: no restraint on tilt, poor long period response, simple

calibration, relatively cheap and small compared to broadband seismometers.

## 1.6.1 Station options

### 1. Stations Located on Structures

A typical current digital strong motion station located on a structure deploys a 24-bit accelerometer recording onto a 16-bit datalogger in a triggered mode. Structures commonly instrumented are buildings, bridges and dams.

Recording of 24-bit data ( $\sim 144dB$ ) would be useful, as evidence from buildings continuously monitored at Caltech indicates that typical building noise levels are similar to the digitiser noise floor for a 16-bit accelerometer station, and a factor of 100 above the instrument noise for a 24-bit instrument. Monitoring structural noise can greatly improve understanding of structural response.

The noise levels at these sites are high enough that a broadband sensor would be redundant, as all motions above the station noise are recorded on-scale by the strong motion instrument. GPS requires an unobstructed view of the sky, so within a building, a roof site is the only option. Further, ambient displacements on structures are often large, which would make GPS noisy, and only be useful for strong motions. GPS may be important if it is used on a free-field site near the structure, where long-term displacements may be more accurately determined, and the free-field displacements from strong motion could be used as input motion to the building system.

The main decisions to consider for a structural station are thus:

**a. Strong Motion Velocity Meter vs. Accelerometer:** A velocity meter has the advantage of increased sensitivity at low frequencies, so more teleseismic and regional events can be recorded - this is especially useful if the station is operated in continuous mode, as these motions would fail to trigger a triggered setup. Transient displacement estimates are more stable as only a single integration is required to obtain displacement with frequencies above  $0.0125Hz$ . Accelerometers, however, have the advantages of being cheaper, smaller, lighter and easier to calibrate.

The FBA type instrument is best suited to a building instrumented with a large array of sensors, which need to be located in small spaces. If the building noise is well below the FBA type instrument noise floor at long periods, the strong motion velocity meter may be a useful option.

**b. Triggered vs. Continuous:** The decision to record data in a triggered mode implies some concern with the cost and time taken by data processing and storage. If a station can be placed within a modern seismic network, such as stations MIK and CBC in the CISN, data can be handled and made available with minimal extra work within the network. The advantages of continuous recording are clear from this thesis, studies of building response to ambient vibrations show the building is a dynamic system sensitive to environmental changes, as well as internal usage. Continuous recording also leads to recordings of small ground motions that would not trigger a system only designed to record large motions. These motions provide insight into building performance, and have obvious potential for a Green's Functions approach for the determination of building response to larger, potentially destructive ground motions.

In summary, for research value, the optimal 24-bit station within a structure would deploy a strong motion velocity sensor recording continuously.

## **2. Low-Noise Station**

A typical field station within a modern broadband seismic network consists of 24-bit data-logger recording the output from both a strong motion FBA sensor and a high-gain broadband velocity sensor.

The high-gain velocity sensor is shown to be capable of recording below the ambient station noise for most station sites over a broad frequency band. Combined with a strong motion sensor, the two instruments effectively cover all ranges of motions from the strongest possible earthquake motions to the station noise level, over a very broad frequency range. The instruments are insensitive to static offsets, and so care must be taken in interpreting strong ground motions with associated static offset. Numerical instability as well as the inability of an inertial sensor to distinguish between ground displacement and

ground tilt cause this problem. One obvious way to measure the permanent displacement accurately is with GPS, which is now capable of recording to millimeter accuracy at  $1\text{ sps}$ . GPS also has no upper bound on the size of displacements that can be recorded.

Co-locating GPS with these very broadband seismic stations would produce a station with a dynamic range that encompasses the full range of earth motions, as well as unambiguously determining station displacements. This is the ideal configuration for a modern network using 24-bit technology.

In some cases within the CISN and in other networks, stations are composed of a single strong motion sensor placed alongside a 24-bit digitiser. This may be a typical configuration within denser urban regions where noise levels are so high they approach the limits of resolution for the strong motions sensors (and consequently little seismic data not recorded by a strong motion sensor would be recorded by a high-gain broadband sensor). In such a station, deploying a strong motion velocity sensor is significantly advantageous to using an FBA sensor, as more long period low amplitude signals, such as teleseisms, will be recorded at the station.

### **3. Adding Seismic Sensors to an Existing GPS Network**

A current topic of interest is adding seismic sensors to existing GPS network stations. The question is what sort of sensors should be used. The goal of adding the new sensors is not to replicate the full-range broadband stations, but to record a broadband timeseries from a large earthquake. This is because technically GPS is limited to  $1\text{ sps}$ , and in any case, it would be insensitive to the small displacements at frequencies higher than  $1\text{ sps}$ . Addition of a strong motion instrument would mean the strong motion is recorded over a very broad frequency band.

The cheapest and simplest configuration would be to add an FBA type instrument operating in triggered mode. If its only aim is to record the strongest ground motions, the digitiser would not need to be 24-bit, 16-bit instruments would suffice. In this mode, the FBA type sensor would be the preferred option as the advantages of a velocity instrument (better high-frequency displacement, increased event resolution) are negated. However, a 24-bit instrument with continuous transmission to a network storage facility would have

many advantages. Firstly, the data from large earthquakes would still be recorded. Also, the existing strong motion network would become denser with a minimum of effort and cost, as the GPS stations are already setup and access rights to the site have already been established. For a network like CISN, this could have important benefits for many of the real-time data analysis and products.

If a continuous strong motion sensor was to be deployed alongside existing GPS, the ideal type would be the strong motion velocity sensor described in detail in this thesis. The increased sensitivity to small regional and teleseismic data makes this instrument a better alternative to the FBA-type sensors.